

Supporting Information

Exploring centimeter-sized single crystal of 2D Dion-Jacobson halide perovskite toward efficient X-ray detection

Yipeng Fan,^{ac} Jiayi Chen,^{ab} Xinping Ouyang,^{ab} and Shuhua Zhang^{*abc}*

a. School of Environment and Energy, South China University of Technology, Guangzhou, Guangdong 510006, P. R. China

b. College of Chemistry, Guangdong University of Petrochemical Technology, Maoming, Guangdong 525000, P. R. China

c. College of Chemistry and Bioengineering, Guilin University of Technology, Guilin, Guangxi, 541004, P. R. China

E-mail: zsh720108@163.com

Experimental Section

Synthesis. **1** was yielded from hydroiodic acid solution (55%~58%, Aladdin) containing stoichiometric amounts of $\text{Pb}(\text{CH}_3\text{COO})_2 \cdot 3\text{H}_2\text{O}$ (99.5%, Aladdin) and (S)-1-(4-Nitrophenyl)ethanamine hydrochloride (98% Aladdin). The saturated solution was heated and stirred at 373 K for 20 min to obtain the clarified solution. Bulk single crystals (SCs) of **1** were grown from saturated solution at 0.5 K/day by temperature cooling method.

Powder X-ray diffraction (PXRD). PXRD of **1** was recorded in an atmospheric environment with a Rigaku MiniFlex diffractometer. Using a step size of 0.02° in the 2θ range of 5° - 40° , the diffraction patterns were collected.

Thermogravimetric analysis (TGA) measurement. TGA was performed on STA449C Thermal Analyzer at temperatures ranging from room temperature to 800°C .

Single-crystal structure determination. On a Bruker 8 diffractometer, single-crystal X-ray diffractions of **1** was carried out using $\text{Mo K}\alpha$ radiation at 150 K. The Crystalclear software program was used to analyze the data. Direct techniques were used to solve the structures of **1**, and the SHELXLTL software was used to refine them using full-matrix least-squares refinements on F^2 .

UV-Vis-NIR Diffuse Reflection Spectroscopy. On a PE Lambda 900 UV-Visible spectrometer, the solid UV absorptions were measured at room temperature.

Computational description. Single-crystal structure data of **1** at 150 K was used for the theoretical calculations. Band structure and partial density of states (PDOS) were performed by the DFT method within the total-energy code CASTEP.

X-ray detection. The I - V traces and I - t curves under X-ray irradiation was also recorded using the 6517B high precision electrometer (Keithley, USA). A commercially available Ag target X-ray tube with X-ray photons energy up to 50 keV and peak intensity at 22 keV was used as the X-ray source (4 W, Mini-X2, Amptek, USA). The dosage rate of X-ray tube was modulated by altering its tube current and measured by a commercial X-ray dosimeter (Accu-Gold, Radcal, USA) attached with the ion chamber (10×6-180 model) in an integrating mode.

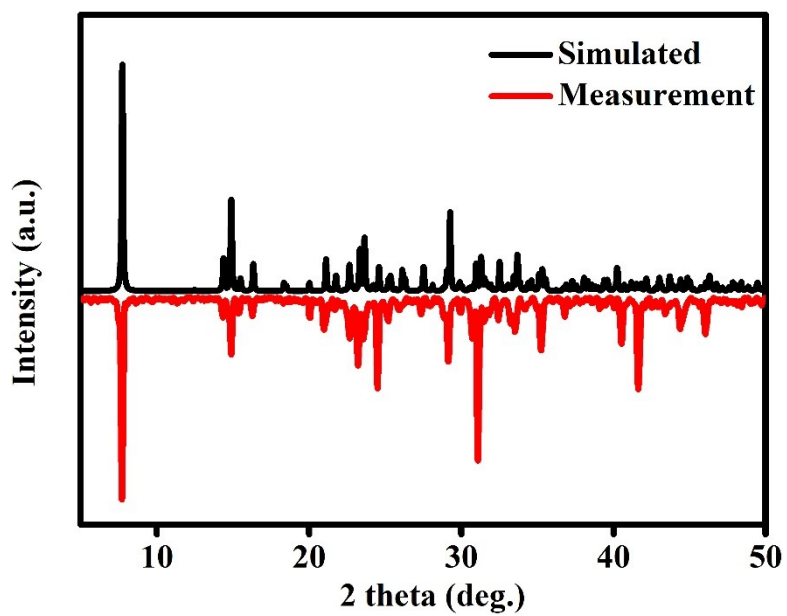


Fig. S1 The simulated and experimental PXRD patterns of 1.

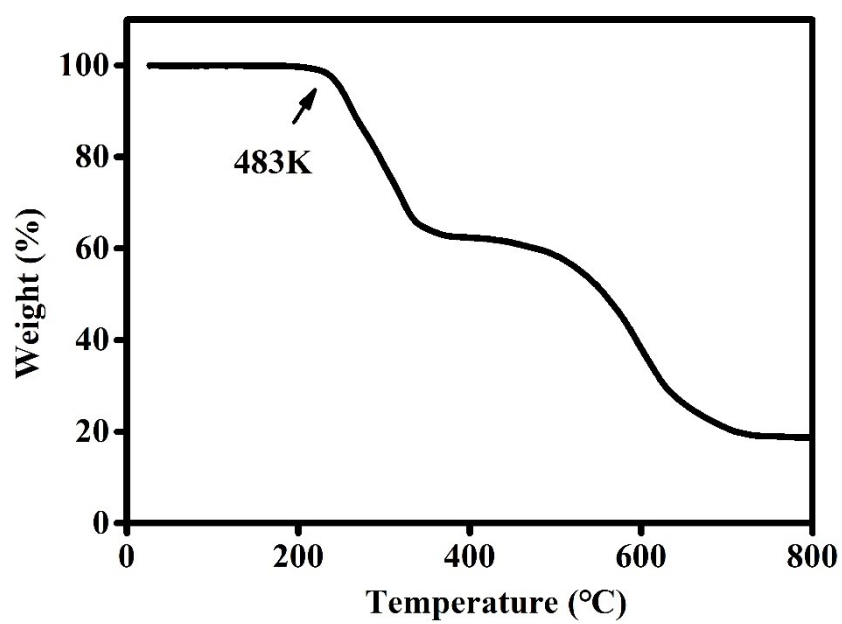


Fig. S2 Thermogravimetric analysis of synthesized 1.

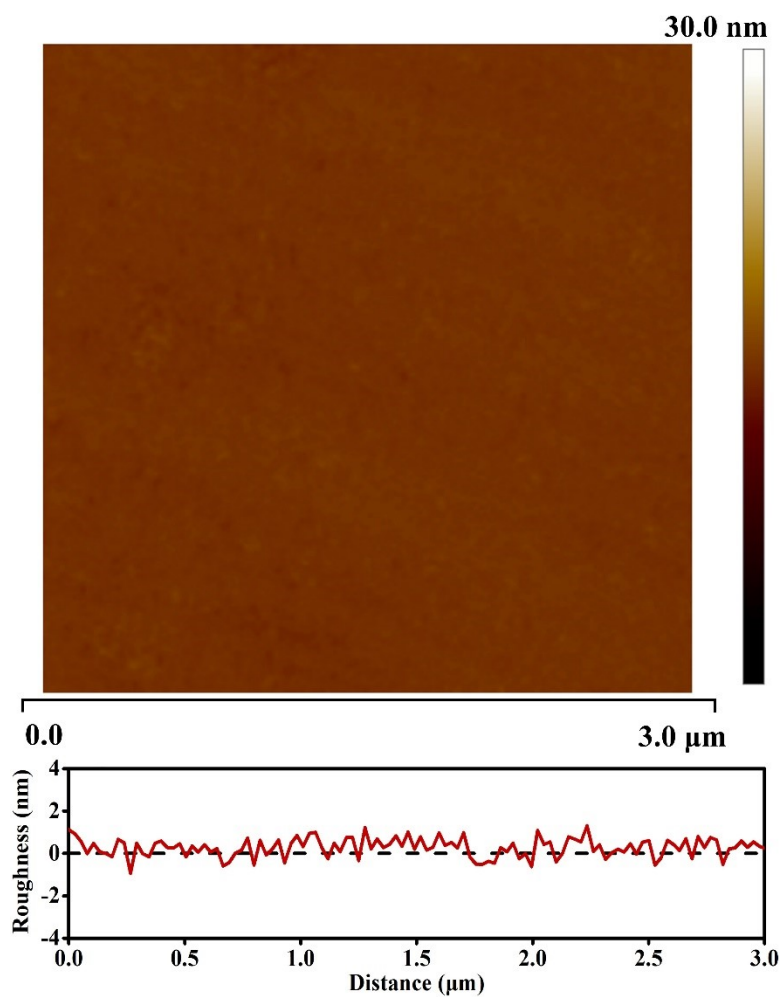


Fig. S3 Surface morphology measured by AFM.

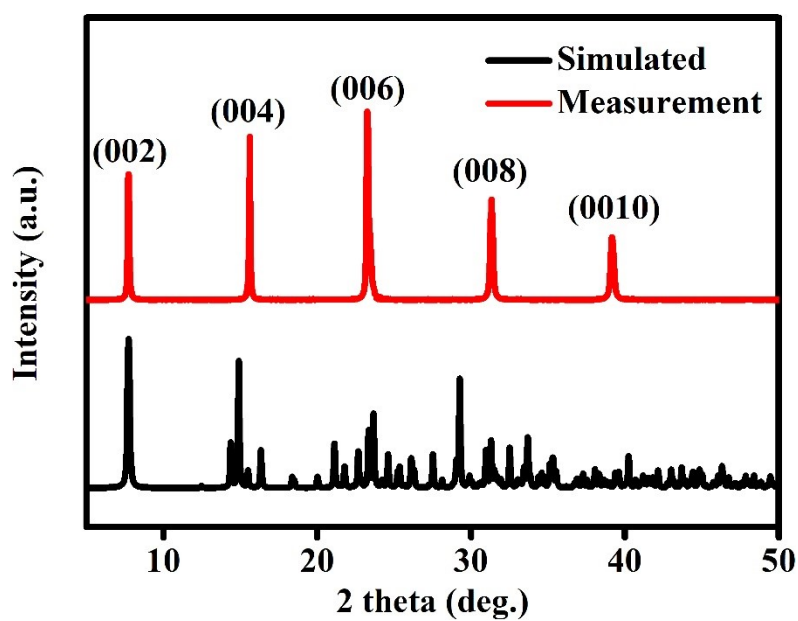


Fig. S4 XRD scan of the top facet of 1 SC.

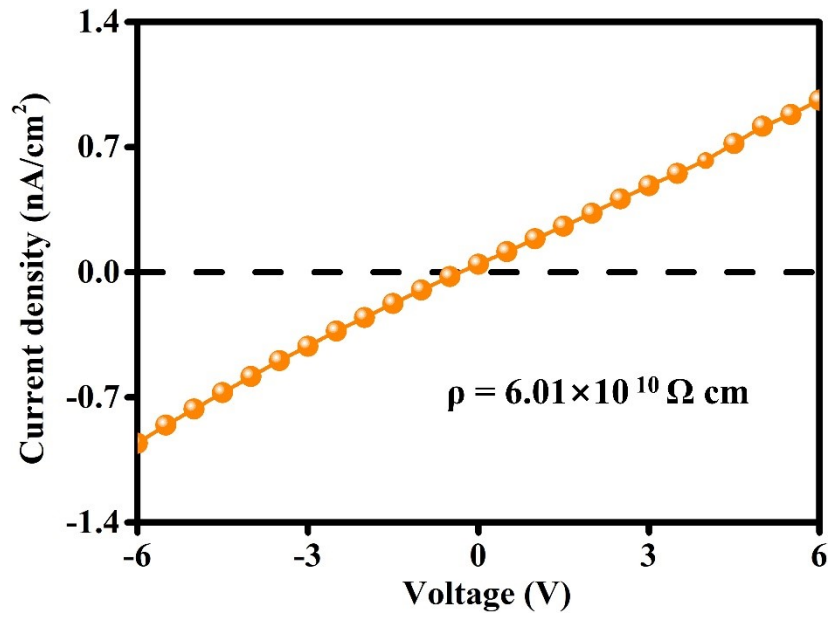


Fig. S5 Bulk resistivity of 1 SC.

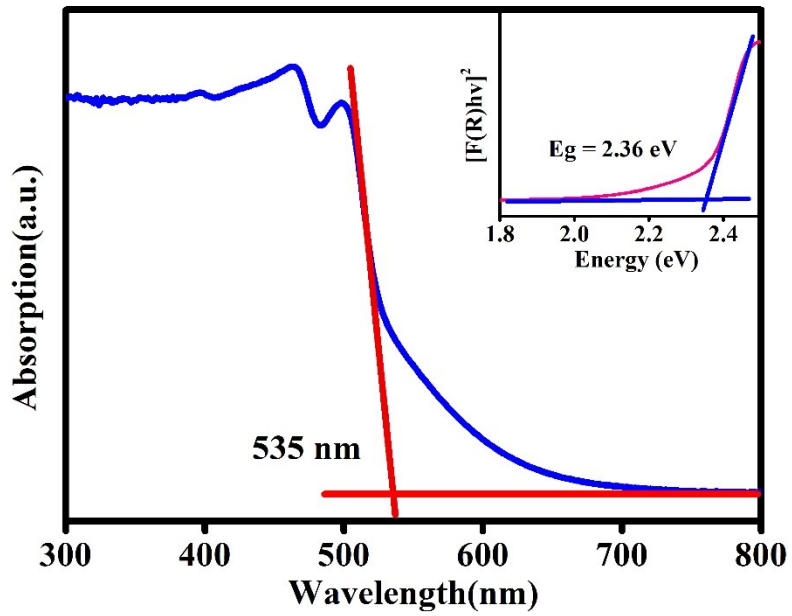


Fig. S6 The absorption spectrum and derived optical bandgap (inset) of 1.

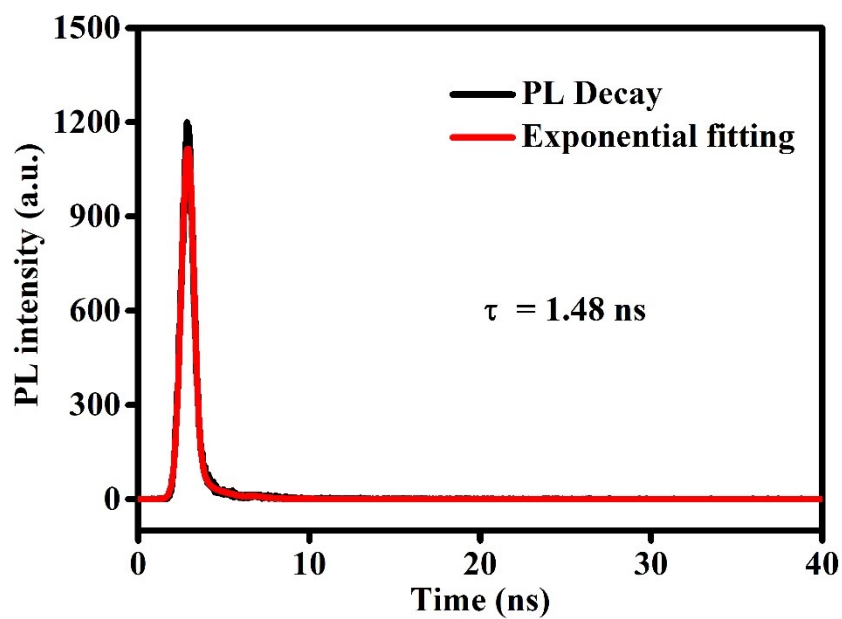


Fig. S7 PL decay curve monitored at 505 nm of **1** SC under 375 nm excitation.

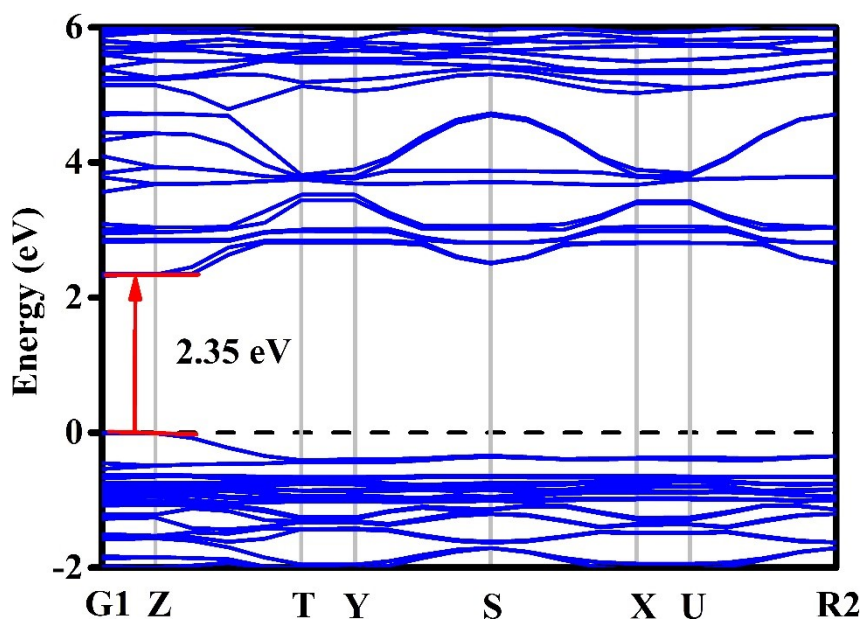


Fig. S8 Calculated band structure of **1**.

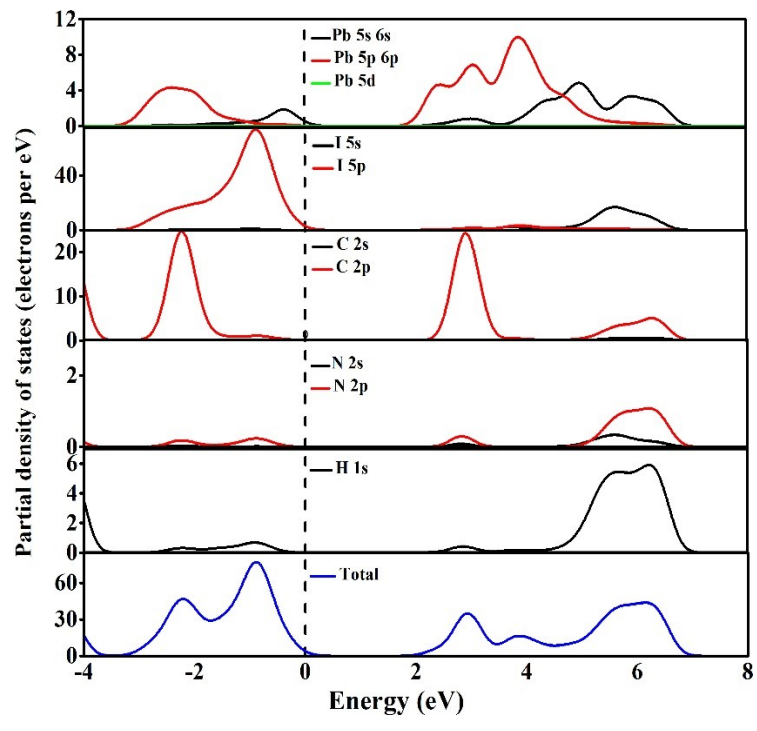


Fig. S9 PDOS spectra of 1.

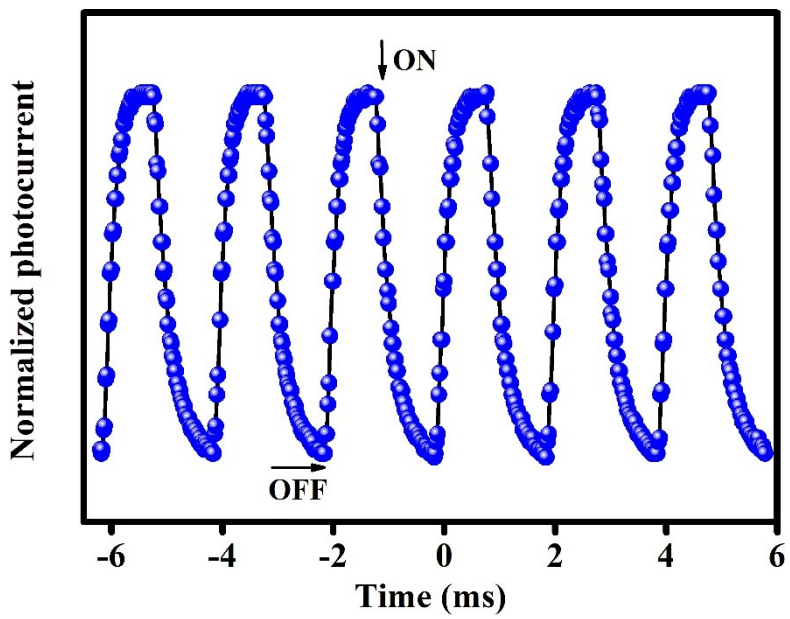


Fig. S10 Repetitive switching cycles of photoresponse for 1.

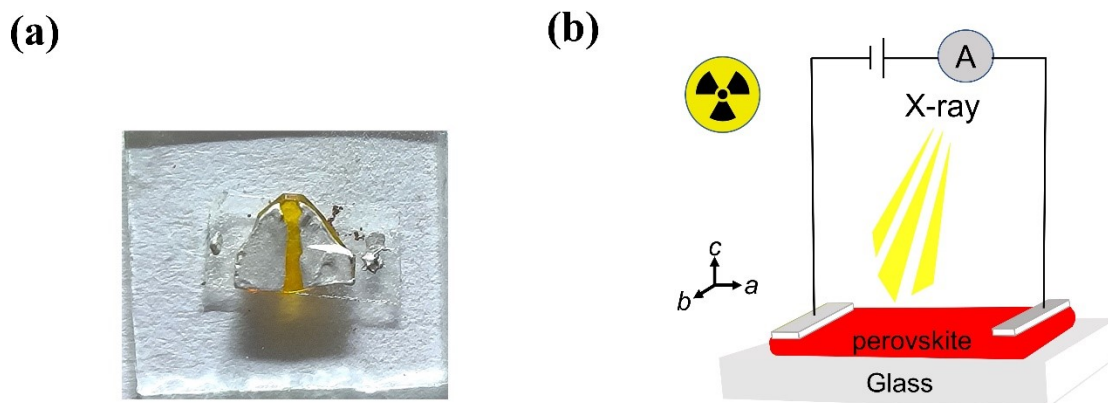


Fig. S11 (a) Device picture based on **1** SC. (b) Schematic illustration of X-ray detection based on **1** SC.

Table S1. Crystallographic data and structure refinements of **1** at 150 K.

Empirical formula	$C_8H_{14}I_4N_2Pb$
Formula weight	853.00
Temperature/K	150
Crystal system	orthorhombic
Space group	$P2_12_12_1$
$a/\text{\AA}$	8.4311(3)
$b/\text{\AA}$	9.0270(4)
$c/\text{\AA}$	22.8714(12)
$\alpha/^\circ$	90
$\beta/^\circ$	90
$\gamma/^\circ$	90
Volume/ \AA^3	1740.69(13)
Z	4
$\rho_{\text{calc}}/\text{cm}^3$	3.255
μ/mm^{-1}	16.766
$F(000)$	1480.0
Radiation	MoK α ($\lambda=0.71073$)
2θ range for data collection/ $^\circ$	4.852 to 54.98
Reflections collected	10425
Data/restraints/parameters	3900/0/139
Goodness-of-fit on F^2	0.969
Final R indexes [$I \geq 2\sigma(I)$]	$R_1 = 0.0321$, $wR_2 = 0.0694$
Final R indexes [all data]	$R_1 = 0.0348$, $wR_2 = 0.0710$
Largest diff. peak/hole/ $e \text{\AA}^{-3}$	1.21/-1.76

Table S2. A detection limit summary of perovskite single-crystal X-ray detectors.

Materials	Operating voltage (or electric field)	Detection limit	detection sensitivity	Ref.
FA ₃ Bi ₂ I ₉	180 V	0.2 $\mu\text{Gy}_{\text{air}} \text{s}^{-1}$	598 $\mu\text{C Gy}_{\text{air}}^{-1} \text{cm}^{-2}$	1
(BDA)PbI ₄	10 V	430 $\text{nGy}_{\text{air}} \text{s}^{-1}$	242 $\mu\text{C Gy}_{\text{air}}^{-1} \text{cm}^{-2}$	2
(R)-(H ₂ MPz)BiI ₅	50 V mm ⁻¹	4.38 $\mu\text{Gy}_{\text{air}} \text{s}^{-1}$	242 $\mu\text{C Gy}_{\text{air}}^{-1} \text{cm}^{-2}$	3
MAPbBr ₃	-20 V	0.48 $\mu\text{Gy}_{\text{air}} \text{s}^{-1}$	2975 $\mu\text{C Gy}_{\text{air}}^{-1} \text{cm}^{-2}$	4
(3AP)PbCl ₄	5 V	1.54 $\mu\text{Gy}_{\text{air}} \text{s}^{-1}$	791 $\mu\text{C Gy}_{\text{air}}^{-1} \text{cm}^{-2}$	5
Cs ₂ AgBiCl ₆	2 V mm ⁻¹	241 $\text{nGy}_{\text{air}} \text{s}^{-1}$	325 $\mu\text{C Gy}_{\text{air}}^{-1} \text{cm}^{-2}$	6
DABCO-N ₂ H ₅ Br ₃	10 V	2.68 $\mu\text{Gy}_{\text{air}} \text{s}^{-1}$	1143 $\mu\text{C Gy}_{\text{air}}^{-1} \text{cm}^{-2}$	7
(BA) ₂ PbI ₄	10 V mm ⁻¹	241 $\text{nGy}_{\text{air}} \text{s}^{-1}$	148 $\mu\text{C Gy}_{\text{air}}^{-1} \text{cm}^{-2}$	8
α -Se	200 V	5.5 $\mu\text{Gy}_{\text{air}} \text{s}^{-1}$	20 $\mu\text{C Gy}_{\text{air}}^{-1} \text{cm}^{-2}$	9
1	5 V bias	236 $\text{nGy}_{\text{air}} \text{s}^{-1}$	270 $\mu\text{C Gy}_{\text{air}}^{-1} \text{cm}^{-2}$	This work

References

- 1 W. Pan, H. Wu, J. Luo, Z. Deng, C. Ge, C. Chen, X. Jiang, W.-J. Yin, G. Niu, L. Zhu, L. Yin, Y. Zhou, Q. Xie, X. Ke, M. Sui, J. Tang, *Nat. Photonics*, 2017, **11**, 726-732.
- 2 Y. Shen, Y. Liu, H. Ye, Y. Zheng, Q. Wei, Y. Xia, Y. Chen, K. Zhao, W. Huang, S. F. Liu, *Angew. Chem., Int. Ed.*, 2020, **59**, 14896-14902.
- 3 S. Tie, W. Zhao, W. Huang, D. Xin, M. Zhang, Z. Yang, J. Long, Q. Chen, X. Zheng, J. Zhu, W. H. Zhang, *J. Phys. Chem. Lett.*, 2020, **11**, 7939-7945.
- 4 B. B. Zhang, X. Liu, B. Xiao, A. B. Hafsia, K. Gao, Y. Xu, J. Zhou, Y. Chen, *J. Phys. Chem. Lett.*, 2020, **11**, 432-437.
- 5 W. Li, D. Xin, S. Tie, J. Ren, S. Dong, L. Lei, X. Zheng, Y. Zhao, W. H. Zhang, *J. Phys. Chem. Lett.*, 2021, **12**, 1778-1785.
- 6 Y. Liu, Z. Xu, Z. Yang, Y. Zhang, J. Cui, Y. He, H. Ye, K. Zhao, H. Sun, R. Lu, M. Liu, M. G. Kanatzidis, S. Liu, *Matter*, 2020, **3**, 180-196.
- 7 B. Xiao, F. Wang, M. Xu, X. Liu, Q. Sun, B.-B. Zhang, W. Jie, P. Sellin, Y. Xu, *CrystEngComm*, 2020, **22**, 5130-5136.
- 8 Q. Xu, C. Li, J. Nie, Y. Guo, X. Wang, B. Zhang, X. Ouyang, *J. Phys. Chem. Lett.*, 2021, **12**, 287-293.
- 9 S. O. Kasap, J. A. Rowlands, *J. Mater. Sci. Mater. Electron*, 2000, 179-198.